Research Article

Journal of Innate Immunity

J Innate Immun 2011;3:420–434
DOI: 10.1159/000322720

Received: April 13, 2010
Accepted after revision: November 14, 2010
Published online: December 18, 2010

# The CD6 Scavenger Receptor Is Differentially Expressed on a CD56$^{dim}$ Natural Killer Cell Subpopulation and Contributes to Natural Killer-Derived Cytokine and Chemokine Secretion

Monika Braun[a, b] Bernadette Müller[b, c] Dominik ter Meer[d] Silke Raffegerst[d, e] Barbara Simm[b] Susanne Wilde[d] Stefani Spranger[d] Joachim Ellwart[d] Barbara Mosetter[d] Ludmila Umansky[b, c] Tina Lerchl[b, c] Dolores J. Schendel[d, e] Christine S. Falk[b, c]

[a]Center for Infectious Medicine, Department of Medicine, Karolinska Institutet, Karolinska University Hospital, Stockholm, Sweden; [b]Immune Monitoring Unit, German Cancer Research Center, National Center for Tumor Diseases, Translational Oncology and Institute for Immunology, University Heidelberg, Heidelberg, [c]Department of Transplantation Immunology, IFB-Tx, Hannover Medical School, Hannover, [d]Institute of Molecular Immunology, and [e]Clinical Cooperation Group Immune Monitoring, Helmholtz Zentrum München, German Research Center for Environmental Health, Munich, Germany

**Key Words**
CD6 · Chemokines · Cytokines · Natural killer cells · Natural killer subpopulations · Scavenger receptor

**Abstract**
The CD6 scavenger receptor is known to be expressed on virtually all T cells and is supposed to be involved in costimulation, synapse formation, thymic selection and leukocyte migration. Here, we demonstrate that CD6 is differentially expressed by a subpopulation of peripheral CD56$^{dim}$ natural killer (NK) cells and absent on CD56$^{bright}$ NK cells. CD56$^{dim}$CD16$^{+}$ cells represent the major NK subset in the periphery, and most cells within this group are positive for CD6. Most killer immunoglobulin-like receptor- and immunoglobulin-like transcript-positive cells also belong to the CD6$^{+}$ subpopulation, as expected from their restricted expression on CD56$^{dim}$ NK cells. In addition, CD6$^{+}$ NK cells are similar to the newly identified CD94$^{low}$CD56$^{dim}$ NK subpopulation and most distant from the recently defined CD27$^{+}$ NK subpopulation based on the reverse correlation of expression between CD6 and CD27, a marker associated primarily with CD56$^{bright}$ NK cells. With respect to CD6 function on NK cells, direct CD6 triggering did not result in degranulation but induced secretion of cytokines (interferon-γ and tumor necrosis factor-α) and chemokines [CXCL10 (IP-10), CXCL1 (GRO-α)]. Thus, CD6 expression on peripheral NK cells marks a novel CD56$^{dim}$ subpopulation associated with distinct patterns of cytokine and chemokine secretion. 

## Introduction

Human natural killer (NK) cells comprise approximately 10–15% of all circulating lymphocytes. They are part of the innate immune system and play a critical role in the host defense against pathogens through produc-

KARGER

Fax +41 61 306 12 34
E-Mail karger@karger.ch
www.karger.com


1662–811X/11/0034–0420$38.00/0

Accessible online at:
www.karger.com/jin

Prof. Dr. rer. nat. Christine S. Falk
Department of Transplantation Immunology, IFB-Tx
Medizinische Hochschule Hannover MHH
Carl-Neuberg-Strasse 1, DE–30625 Hannover (Germany)
Tel. +49 511 532 9745, Fax +49 511 532 8044, E-Mail falk.christine@mh-hannover.de

tion of cytokines and cytotoxicity. Human peripheral NK cells can be divided into 2 major subsets based on the cell surface density of CD56 ($CD56^{dim}$ and $CD56^{bright}$), with each group displaying distinct phenotypic properties. This includes expression of the Fcγ receptor IIIa (CD16), which is present almost exclusively on $CD56^{dim}$ cells, as well as the expression of different repertoires of chemokine receptors and adhesion molecules that foster different migratory capacities [1, 2].

In addition to distinct phenotypic features, these 2 NK subsets have also been associated with different effector functions, suggesting that they play different roles in immune responses. The well-known view that $CD56^{dim}$ NK cells are primarily responsible for cytotoxic activity, including CD16-mediated antibody-dependent cellular cytotoxicity, is currently revisited due to the definition of more NK subsets with different cytotoxic potential. Along this line, $CD56^{bright}$ NK cells are postulated to regulate immune responses primarily through their cytokine production, for example by secretion of interferon (IFN)-γ after stimulation with interleukin (IL)-2, IL-12 or IL-15 [3]. However, a sharp functional assignment of these 2 major phenotypes to cytotoxicity or cytokine secretion seems to be too simplistic.

Since their phenotypic characterization, it has been postulated that peripheral blood $CD56^{bright}$ and $CD56^{dim}$ NK cells represent 2 sequential stages of terminal NK cell maturation, albeit it is still under debate which phenotype represents the more differentiated state. It has been shown in several studies that $CD56^{bright}$ NK cells can differentiate into $CD56^{dim}$ NK cells [4, 5], but the reverse differentiation of $CD56^{dim}$ into $CD56^{bright}$ cells has also been observed [6]. Recently, the surface density of the C-type lectin receptor CD94 that forms heterodimers either with NKG2A or NKG2C was assigned to developmental stages in correlation with the $CD56^{bright/dim}$ NK subsets. The progression is postulated to occur in peripheral NK cells from $CD94^{high}CD56^{bright}$ to $CD94^{high}CD56^{dim}$ and further to $CD94^{low}CD56^{dim}$ NK cells [7]. This phenotypical division of the $CD56^{dim}$ subset is accompanied by a functional heterogeneity, whereby the $CD94^{high}CD56^{dim}$ NK cells share features of both subsets.

In the current study, we identified CD6, a type B scavenger receptor, as a surface marker that is differentially expressed on $CD56^{dim}$ NK cells. CD6 is primarily expressed on T cells and binds the activated leukocyte cell adhesion molecule, ALCAM (CD166) [8, 9]. Microarray studies revealed CD6 mRNA expression in peripheral NK cells [10]; however, the actual pattern of CD6 protein expression in peripheral NK cells and its impact on function has not been reported to date.

With a detailed evaluation of the phenotype and function of peripheral blood NK cells, we could show here for the first time that CD6 defines a novel NK subpopulation within the $CD56^{dim}$ subset that comprises most of the killer immunoglobulin (Ig)-like receptor-positive ($KIR^+$) and Ig-like transcript-positive ($ILT2^+$) NK cells. We found an inverse distribution of CD6 compared with CD62L and CD27, 2 recently described markers of NK cell subpopulations [11–13]. Moreover, there is a diminished expression of CD94 in the $CD6^+CD56^{dim}$ NK cells which indicates a correlation of this subset to the recently defined $CD56^{dim}CD94^{low}$ NK cells that are postulated as the most differentiated NK cell stage [7]. Direct CD6-mediated triggering did not induce NK cell degranulation but resulted in secretion of pro-inflammatory cytokines and chemokines. Thus, the $CD56^{dim}CD6^+$ NK cells may play a particular role within the $CD56^{dim}$ subset in orchestrating the innate microenvironment.

## Material and Methods

*Peripheral NK Cells*

The collection of blood from healthy donors was approved by the local institutional review board of the Medical Faculty of the Ludwig-Maximilians University Munich and donors gave informed consent. Peripheral NK cells were analyzed using fresh or cryopreserved peripheral blood mononuclear cells (PBMC) of healthy donors, following Ficoll separation, with or without prestimulation with IL-2. Flow cytometric analysis of PBMC composition was performed in parallel with degranulation experiments and stimulation with plate-bound monoclonal antibodies (mabs). For some experiments, isolation of $CD56^{dim}$ and $CD56^{bright}$ NK cells was performed using MACS separation kits (Miltenyi, Bergisch Gladbach, Germany). For FACS sorting of NK cell fractions, PBMC were enriched for NK cells using an NK-negative isolation kit (Dynal; Invitrogen, Carlsbad, Calif., USA). Isolated NK cells were stained with CD6-FITC (MEM-98, Biozol), CD3-PerCP (clone SK7; Becton Dickinson, San Jose, Calif., USA) and CD56-PE (clone NKH-1; Beckman Coulter, Fullerton, Calif., USA) mabs. Gates were first set for $CD56^+CD3^-$ NK cells and subsequently for the $CD6^+$ or $CD6^-$ subpopulations using a FACSAria (Becton Dickinson). Following sorting, NK subpopulations were directly used for isolation of mRNA, for stimulation with IL-2 or IL-15 or tested for cytotoxicity in 4-hour standard chromium release assays after a 24-hour resting time.

*Stimulation of NK Cells via Plate-Bound Mabs*

For the mab-specific stimulation of NK cells used to study degranulation or cytokine release, 96-well plates were coated with anti-mouse $F(ab)_2$ fragments, 20 μg/ml in borate buffer (0.05 M, pH = 8), overnight at 4°C. After 2 washing steps with PBS, secondary mabs against CD3 (clone OKT3; BioLegend, San Diego, Calif.,

USA), CD6 clone MT-606 (IgG2b; Baxter, Unterschleißheim, Germany), clone MEM-98 (IgG1; BioLegend), clone BL-CD6 (IgG1; BioLegend) or isotype control (clone MOPC21, IgG1; Sigma, Deisenhofen, Germany) were added (10 μg/ml in PBS with 1% FBS), incubated for 30 min at 4°C, followed by 2 washing steps with PBS. $CD56^{bright}$ or $CD56^{dim}$ NK cells ($5 \times 10^4$ and $3 \times 10^5$, respectively) were incubated for 48 h in 200 μl RPMI-1640, 1 mM sodium pyruvate, 2 mM L-glutamine, non-essential amino acids (all from Gibco/Invitrogen/Life Technologies, Carlsbad, Calif., USA) 10% human serum and 100 U/ml IL-2 (Proleukin; Cetus, Emeryville, Calif., USA). The supernatant was harvested and analyzed for cytokine content by the multiplex technology. To determine degranulation, IL-2-activated PBMC were incubated with plate-bound mabs for 4 h without IL-2, and CD107a expression was analyzed on NK cells by flow cytometry after gating for $CD56^+CD3^-$ cells. For intracellular cytokine staining (ICS), PBMC were stimulated with plate-bound mab for 6 h with or without IL-2 (500 U/ml) and analyzed with the ICS staining protocol (see below).

*Immunophenotyping of NK Cells*

The following mabs were used for cell surface staining by multi-color flow cytometry: CD3-PerCP (clone SK7), CD6-PE (clone M-T605), LAIR-1-PE (clone DX26), CD62L-FITC (clone SK11), CD27-APC (clone L128), CD94-FITC (HP3D9), CD57-FITC (clone NK-1; all from Becton Dickinson), NKG2D-PE (clone 149810; R&D Systems, Minneapolis, Minn., USA), CD6-FITC (MEM-98; Biozol), CD16-FITC (clone 3G8), CD56-APC (clone NKH-1), CD94-PE (clone HP-3B1), NKG2A-PE (clone Z199), KIR2DL/S1-specific p58.1-PE (clone EB6), KIR2DL/S2,3-specific p58.2-PE (clone GL183), KIR3DL1-specific p70-PE (clone Z27.3.7), KIR2DS4-specific p50.3-PE (clone FES172), NKp30-PE (clone Z25), NKp44-PE (clone Z231), NKp46-PE (clone BAB281) and ILT2-PE (clone HP-F1; all from Beckman Coulter). Unlabeled CD6 mabs MEM-98, BL-CD6 and MT-606 were compared in combination with PE-labeled secondary goat α-mouse mab. Unlabeled mab against KLRG1 was kindly provided by H.P. Pircher (University Freiburg, Germany) and also used in combination with PE-labeled secondary goat α-mouse mab. Isolated PBMC were incubated with mabs for 30 min on ice, washed with PBS with 2.5% FBS and 0.1% sodium azide and fixed with PBS containing 1% paraformaldehyde. Cells were analyzed using flow cytometry (FACSCalibur, LSRII or FACSAria; Becton Dickinson). Data were processed using CellQuest-Pro software 5.2.1 and FACSDiva software 5.0.2 (Becton Dickinson) or FlowJo software (version 8.8.1–8.8.4; Tree Star, Ashland, Oreg., USA).

*Cytotoxicity and Degranulation Assays*

NK cells were sorted according to their expression of CD56 and CD6 and used as effector cells in standard 4-hour chromium release assays. After labeling with $^{51}NaCrO_4$ for 60 min at 37°C, the target cells were incubated with NK cells in duplicate samples in 4-step titrations, starting with an effector to target cell ratio (E:T) of 10:1. The supernatant was harvested after 4 h of coincubation, and spontaneous as well as maximum release were used to calculate percentages of specific cytotoxicity using the following formula: % specific cytotoxicity = [(experimental cpm – spontaneous cpm)/(total cpm – spontaneous cpm)] × 100.

Specific activation of NK cell subsets was quantified using a FACS-based CD107a degranulation assay. For this, PBMC were cultured for 48 h in RPMI-1640, 1 mM sodium pyruvate, 2 mM L-glutamine, non-essential amino acids, 10% FBS and 500 U/ml IL-2 (Proleukin, Cetus). These prestimulated PBMC were incubated for 4 h at 37°C with target cells (E:T = 1:1) or specific plate-bound mabs and 10 μl FITC- or PE-labeled CD107a mab (clone H4A3; Becton Dickinson) in a final volume of 200 μl. To detect spontaneous degranulation, samples without target cells were included in every experiment. After 1 h of incubation, 5 μl monensin [2 mM, in EtOH (50% v/v)/RPMI-1640; Sigma] were added to prevent quenching effects. After washing with PBS, counterstaining of the NK cells was performed with CD3-PerCP (clone SK7), CD56-APC (clone NKH-1) and CD6-PE (clone M-T605) mabs. FACS data were analyzed using CellQuest-Pro and Diva software and quantified by applying Boolean mathematics.

The following human leukocyte antigen (HLA) class I negative target cells were used in cytotoxicity and degranulation assays: L721.221, K562 and Daudi. The HLA-E transfectant of K562, K562-E (clone 2B4), was generated as previously described [14–16], and the expression of HLA-E was analyzed concomitant to all cytotoxicity analyses.

*Cytokine Detection in NK Cell Culture Supernatants*

Cytokine and chemokine concentrations in supernatants of separated and mab-stimulated NK cells were quantified by multiplex protein arrays, according to the manufacturer's instructions (BioRad Laboratories, Hercules, Calif., USA). A 2-laser array reader (Bio-Plex System; BioRad Laboratories) simultaneously quantifies all cytokines and chemokines of interest. Standard curves and concentrations were calculated with Bio-Plex Manager 4.1.1 on the basis of the 5-parameter logistic plot regression formula. The detection sensitivity of all analytes was between 2 and 10 pg/ml.

*Intracellular Cytokine Staining*

For intracellular staining, PBMC were resuspended in PBS containing 2.5% FCS and 0.1% $NaN_3$ (staining buffer) and stained with directly labeled antibodies directed against CD56, CD3, CD16 or CD6 at 4°C. After 20 min, cells were washed once in staining buffer, fixed with 1.5% paraformaldehyde (AppliChem, USA) for 5 min at room temperature and washed once again with staining buffer. To detect intracellular cytokines/chemokines, cells were permeabilized with staining buffer containing 0.05% saponin (Roth, Germany) for 5 min at room temperature and finally incubated with anti-cytokine/chemokine antibodies IFN-γ-PE (BD Pharmingen; clone B27, mouse IgG1), tumor necrosis factor (TNF)-α-Alexa Fluor 647 (BioLegend; clone MAb11, mouse IgG1) and CXCL10-PE (R&D Systems; clone 33036, mouse IgG1) for 20 min at room temperature. After 1 washing step, cells were resuspended in staining buffer. The fluorescence was analyzed by flow cytometry as described above. Isotype-matched antibodies were used to control for non-specific staining.

*Chemokine-Induced NK Cell Migration*

PBMC ($4 \times 10^5$) in 100 μl RPMI-1640 supplemented with 1 mM sodium pyruvate, 2 mM L-glutamine, non-essential amino acids and 0.5% BSA (Roth) were placed in the upper chamber of 24-well Transwell plates with 5-μm pores (Costar, Cambridge, Mass., USA). The following recombinant chemokines were placed into the lower chamber in a volume of 600 μl of the same migra-

tion medium at a concentration of 100 ng/ml: CXCL10, CCL5, CXCL12, CXCL1 or CXCL8 (Immunotools, Germany). After incubation at 37°C for 4 h, cells that migrated into the lower chamber were harvested and stained with antibodies directed against the cell surface markers CD56, CD3, CD16 and CD6, as described above. To quantify the number of migrated cells, 30 μl 100× prediluted BD™CompBeads were added to each sample directly before flow cytometry. 5,000 events were acquired in the bead gate in order to determine the cell number in each sample. The migrated cells were calculated according to the background, i.e. cells migrating randomly in medium alone, which results in the migration index (x-fold increase). All conditions were performed in triplicates (±SEM).

*CD6 Gene Expression of Sorted NK Cell Fractions*

RNA from sorted NK cell subpopulations was isolated using the RNeasy kit (Qiagen, Hilden, Germany) following the manufacturer's protocol. Total RNA (1 μg) was reverse transcribed utilizing the AffinityScript QPCR cDNA Synthesis kit (Stratagene, La Jolla, Calif., USA). Amplification of CD6 transcripts was performed by RT-PCR on a LightCycler (LC) instrument (Roche, Basel, Switzerland) using the LC FastStart DNA Master$^{Plus}$ SYBR Green I kit using 1 μl of template cDNA and 10 pmol of each primer. CD6 forward primer 5′-TCTGTCCACTCCCGAAGTCC-3′ and CD6 reverse primer 5′-GATGGTGGTGGGTAGGTGCT-3′ annealed to positions 5′1326 to 3′1558 (NCBI NM_006725.3) and yielded a product of 232 bp. From each fraction, a control was performed with the 18S rRNA housekeeping gene, amplified with the following primers: 18S forward primer 5′-CGGCTACCACATCCAAGGAA-3′ and 18S reverse primer 5′-GCTGGAATTACCGCGGCT-3′ (187 bp). LC-PCR conditions used an initial denaturation at 95°C for 10 min followed by 35 cycles at 95°C for 0 s, annealing at 58°C for 25 s and elongation at 72°C for 25 s, followed by standard gel electrophoresis.

*Statistics*

For statistical evaluation, the GraphPad PRISM 5 software was utilized. The unpaired t test and, for non-parametric data sets, Mann-Whitney U statistical tests were applied, respectively.

## Results

*CD6 Differentiates Subpopulations of Peripheral NK Cells*

Peripheral NK cells of 17 healthy donors were analyzed by flow cytometry for the expression of CD6, in combination with CD16 and CD56, whereby 3 CD6-specific mabs gave identical results (online suppl. fig. 1A, www.karger.com/doi/10.1159/000322720). As expected, the majority of CD56$^{dim}$ NK cells expressed high levels of CD16 (Fcγ receptor III), whereas CD56$^{bright}$ cells expressed little or no CD16 (fig. 1a, c). Interestingly, CD6 was differentially expressed on a fraction of CD56$^{dim}$ cells, with a significantly higher percentage of CD56$^{dim}$CD6$^{+}$ compared with CD56$^{dim}$CD6$^{-}$ NK cells ($p < 0.0001$; fig. 1), whereas only a few CD56$^{bright}$ cells were CD6$^{+}$ (fig. 1a, c). Thereby, CD6 delineated 2 groups of NK cells: 71.7% were CD6$^{+}$ (70.5 ± 11.7% CD56$^{dim}$, 1.2 ± 0.8% CD56$^{bright}$) and 28.3% were CD6$^{-}$ (22.9 ± 10.3% CD56$^{dim}$, 5.4 ± 2.2% CD56$^{bright}$; fig. 1c). Accordingly, CD56$^{dim}$CD16$^{+}$CD6$^{+}$ cells represent the main NK cell subpopulation in the periphery. In sorted CD6$^{-}$CD56$^{dim}$ NK cells (subset B), it was not possible to induce CD6 expression in vitro within 5 days of culture in the presence of IL-2 or IL-15, whereas CD6 expression on sorted CD6$^{+}$CD56$^{dim}$ NK cells remained stable after cytokine stimulation (online suppl. fig. 2A). In CD16 positively selected NK cells, the CD6$^{+}$CD16$^{+}$CD56$^{dim}$ NK cells (subset A) decreased but did not develop into the CD56$^{bright}$ NK cells following cytokine stimulation (online suppl. fig. 2B). Instead, CD16$^{-}$CD56$^{low}$CD6$^{low}$ NK cells expanded within 8 days, indicating that this CD16-based positive selection procedure is followed by downmodulation of several receptors within 2 days in the presence of cytokines.

*NK-Associated Surface Markers Vary on CD56$^{dim}$ Subsets Differentiated by CD6*

Due to the very small number of CD56$^{bright}$CD6$^{+}$ NK cells, they were not considered further as a distinct NK cell subpopulation. Therefore, phenotyping for CD6 in combination with CD56 divided peripheral NK cells into 3 fractions, with a majority of NK cells being CD56$^{dim}$CD6$^{+}$ (fraction A), followed by CD56$^{dim}$CD6$^{-}$ (fraction B) and CD56$^{bright}$CD6$^{-}$ (fraction C) cells (fig. 1a, right panel). While the numbers of NK cells in each fraction varied among healthy donors (e.g. donors I–III), the distinction of the 3 groups could be easily made in each sample (fig. 1b). Based on this gating strategy, the 3 fractions were compared for expression of a variety of NK-associated markers (fig. 2; online suppl. table 1). Analysis of the density of CD94 expression revealed that all CD56$^{bright}$CD6$^{-}$ NK cells were highly positive for this marker, whereas a slightly lower expression was observed for CD56$^{dim}$CD6$^{-}$ NK cells, which was further decreased on the CD56$^{dim}$CD6$^{+}$ NK cell fraction ($p < 0.0001$ for each comparison; fig. 2a, b). This pattern nicely correlates with the NKG2A expression, the heterodimeric partner of CD94 ($p < 0.0001$ for each; fig. 2a, b). A similar variation in density was seen for the activating NKG2D receptor, which was also reflected in higher expression levels on CD56$^{bright}$CD6$^{-}$ NK cells. The inhibitory LAIR-1 receptor that interacts with collagen [17] was uniformly expressed on essentially all NK cells. The 3 members of the natural cytotoxicity receptor family of activating re-

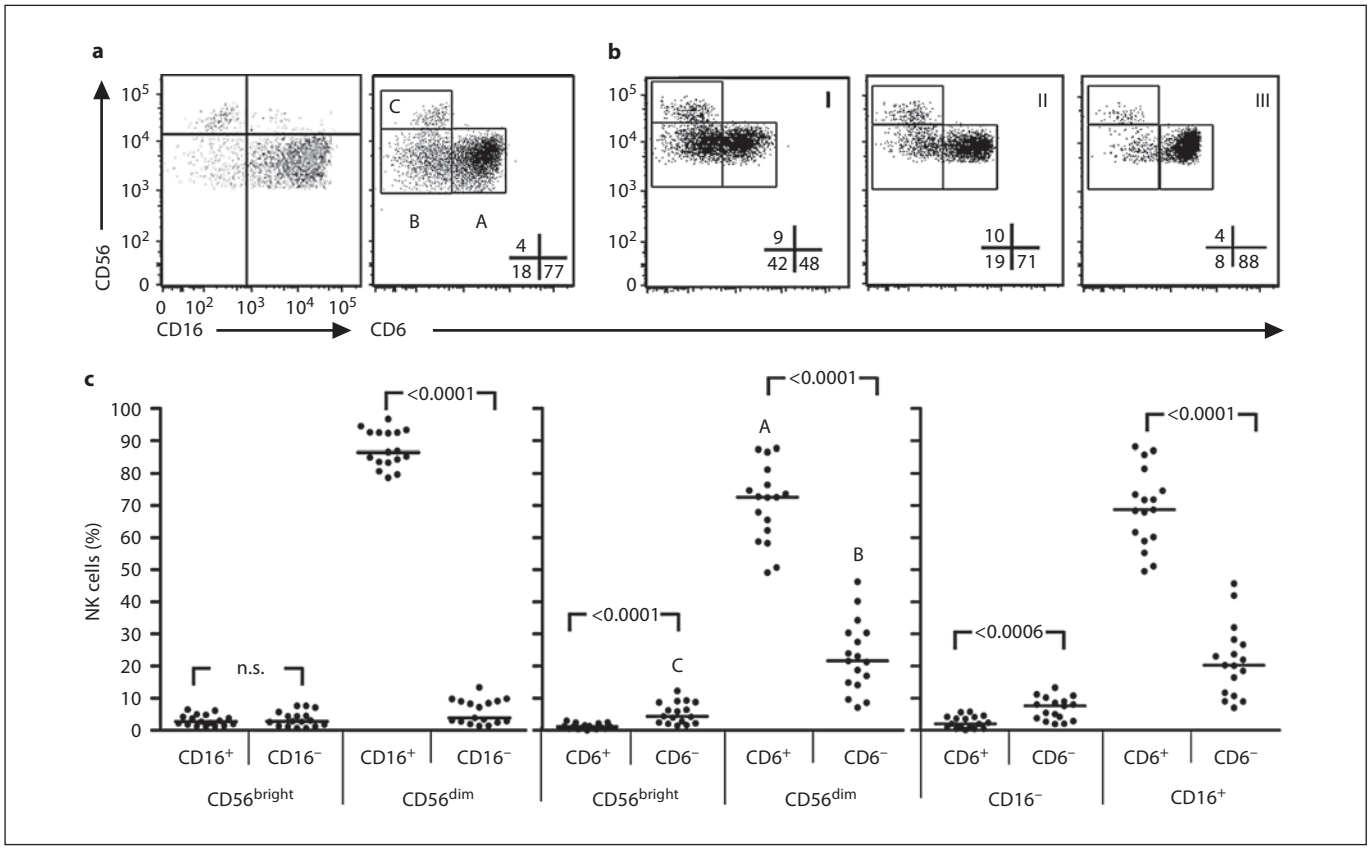


**Fig. 1.** CD6 is differentially expressed on $CD56^{dim}$ NK cells. **a** Peripheral NK cells (gated on $CD56^{+}CD3^{-}$ cells) are divided into 2 major subsets according to the density of their CD56 and CD16 expression, i.e. $CD56^{bright}CD16^{-}$ and $CD56^{dim}CD16^{+/-}$ NK cells. CD6 expression further subdivides $CD56^{dim}$ NK cells into $CD56^{dim}CD6^{+}$ (fraction A) and $CD56^{dim}CD6^{-}$ (fraction B) subpopulations; $CD56^{bright}$ NK cells are $CD6^{-}$ (fraction C). Data are representative for 1 of 17 healthy donors. **b** The distributions of $CD6^{+}$ and $CD6^{-}$ NK cells show donor-specific variations. Examples of NK cells in PBMC of 3 donors (I–III) demonstrate the variability in CD6 and CD56 expression with increasing numbers of $CD56^{dim}CD6^{+}$ cells. **c** $CD56^{dim}CD6^{+}CD16^{+}$ NK cells dominate the peripheral NK cell repertoire. NK cells of 17 healthy donors were examined for CD16, CD56 and CD6 expression. The combined expression of these markers is given as percentages of all $CD3^{-}CD56^{+}$ NK cells. Each data point indicates 1 donor, and the median values are depicted as black bars.

ceptors were distributed almost equally within the 3 fractions. As expected, most NK cells stained positively for the constitutively expressed receptors, NKp46 and NKp30, irrespective of CD6 expression (fig. 2c). The greatest difference was observed between the $CD56^{bright}CD6^{-}$ and the $CD56^{dim}CD6^{+}$ NK subset, whereby the $CD56^{bright}$ NK fraction expressed NKp46 and NKp30 at higher densities. As expected for non-activated NK cells, all fractions were essentially negative for the NKp44 receptor, whose expression is only upregulated following cytokine stimulation [18, 19]. Only the $CD56^{bright}CD6^{-}$ subset showed some NKp44 expression (10.4%) which was also observed for the $CD94^{high}CD56^{bright}$ fraction [7].

The lymphocyte homing receptor CD62L, which is important for migration and adhesion, was most prevalent on $CD56^{bright}CD6^{-}$ cells, but only expressed by lower percentages of the other 2 NK cell fractions (fig. 2d). CD27, a TNF receptor family member that was recently shown to distinguish NK subpopulations with different functions [11] was expressed by about 80% of $CD56^{bright}CD6^{-}$ cells, whereas basically no expression was detected on $CD56^{dim}CD6^{+}$ NK cells (fig. 2d). In contrast, KLRG1 was equally high expressed on population A ($CD6^{+}CD56^{dim}$, 77%) and B ($CD6^{-}CD56^{dim}$, 74%) NK cells but only found on a small proportion of $CD6^{-}CD56^{bright}$ NK cells (fig. 2d). A different distribution could be detected for CD57, a marker that was re-

cently described in the context of NK cell maturation/differentiation [20, 21]. CD57 was significantly higher expressed on subset A (39%) than on subset B (14%) and absent on subset C (fig. 2d). This pattern is similar to KIR and ILT that are expressed primarily on $CD56^{dim}$ NK cells [2]. Therefore, we analyzed the distribution of $KIR^+$ and $ILT2^+$ NK cells in all NK cell fractions. Variable but prevalent expression of KIR and ILT2 was found on $CD56^{dim}CD6^+$ cells, followed by $CD56^{dim}CD6^-$ cells, while essentially no expression was seen on $CD56^{bright}$ $CD6^-$ cells (fig. 2e).

*CD6 Transcript Expression Correlates with Surface Phenotype*

To assess the status of CD6 expression at the transcript level, NK cells were enriched from PBMC and then sorted by flow cytometry to yield the 3 fractions $CD56^{dim}CD6^+$ (subset A), $CD56^{dim}CD6^-$ (subset B) and $CD56^{bright}CD6^-$ (subset C). The sorting gates were stringently defined to avoid contamination with cells falling in the border regions (fig. 3a). Recovered cells were analyzed for CD6 transcripts by qRT-PCR, using the 18S rRNA housekeeping gene as a quantitative and qualitative control (fig. 3b, upper panel). CD6 transcripts were present in the starting PBMC (lane I) as well as in the NK-depleted cell fraction (lane II; fig. 3b, lower panel). These results were expected since CD6 is expressed by T lymphocytes. CD6 transcripts were also present in NK-enriched cells (lane III) that contained all NK cell fractions. When the 3 NK fractions were compared after sorting, CD6 transcripts were only detected in fraction A that comprised the $CD56^{dim}$ $CD6^+$ NK cells (fig. 3b, lower panel). Several CD6 splice variants in extracellular and cytoplasmic domains have been described for T cells [22, 23]. In freshly isolated as well as in IL-2-activated NK cells, these splice variants were also detected, suggesting a similar CD6 mRNA regulation in T and NK cells (online suppl. fig. 1B). Thus, CD6 transcript expression directly correlated with CD6 surface phenotype. These results also demonstrated that the sorting procedure allowed the 3 NK fractions to be cleanly isolated for further functional studies.

*Cytotoxic Capacity of NK Cell Subsets Correlates with the $CD56^{dim}$ Phenotype, but Not with CD6 Expression*

Sorted NK cell fractions isolated by the gating strategy described in figure 3a were analyzed without prior activation for their cytotoxic activity directed against HLA class I negative K562 target cells. A transfectant line of K562 expressing HLA-E (K562-E) was tested in parallel to assess the capacity of the isolated NK cells to respond to inhibitory signals via their NKG2A/CD94 receptors, which were present on substantial numbers of all 3 NK fractions (fig. 2b). Cytotoxic activity was assessed in a standard 4-hour chromium release assay. Sorted NK cells were rested in medium for 24 h prior to the assay. Representative data of 2 unrelated healthy donors, whose NK cells varied somewhat in maximum activity levels, showed the same general pattern (fig. 3c). Both fractions of $CD56^{dim}$ NK cells lysed K562 cells, irrespective of their CD6 expression. Both fractions also responded to NKG2A/CD94-mediated inhibitory signals, as shown by the strong resistance of K562-E target cells to NK-mediated cell lysis. As expected, $CD56^{bright}CD6^-$ cells showed no or low cytotoxic activity which, when detected, was also completely inhibited by HLA-E.

*CD6 Does Not Influence Degranulation of Activated NK Cells*

The direct cytotoxicity assays were performed using freshly isolated NK cells without preactivation with IL-2. To determine if activation would alter these functional patterns, CD107a degranulation assays were performed using IL-2-stimulated NK cells. Degranulation was measured by flow cytometry via detection of CD107a present on the NK cell surface after 4-hour coincubation with 3 target cells, K562, L721.221 and Daudi. Costaining with CD56 and CD6 allowed separate evaluation of the 3 NK fractions as outlined in figure 4a, b. Data from 1 representative analysis of 13 donors is shown in figure 4a, b, wherein sequential gating was applied first to all $CD56^+CD3^-$ NK cells and subsequently combined with CD6 expression (fig. 4a) or CD56 intensity (fig. 4b). NK cells of all gated populations, including the $CD6^+$ and $CD6^-$ fractions as well as the $CD56^{dim}$ and $CD56^{bright}$ subsets, showed degranulation upon incubation with any of the 3 target cells. The degranulation patterns for the 13 healthy donors are summarized in figure 4c and reveal that the distinction of $CD56^{dim}$ NK cells on the basis of CD6 expression had no statistically significant impact on degranulation against these 3 target cells ($p > 0.2$). Furthermore, the comparison of the target cells indicated no significant impact through expression of the CD6 ligand ALCAM (CD166) on degranulation of $CD6^+$ versus $CD6^-$NK cell fractions. This was shown by the detection of comparable levels of CD107a expression by both $CD56^{dim}CD6^+$ and $CD56^{dim}CD6^-$ subsets after activation through $ALCAM^+$ (Daudi, L721.221) and $ALCAM^-$ (K562) target cells.

The lack of impact of CD6 on degranulation was further supported by the finding that direct stimulation of

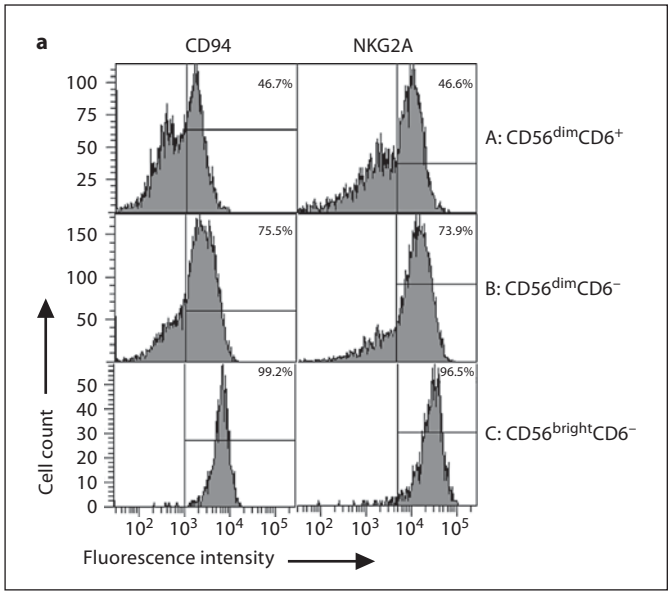


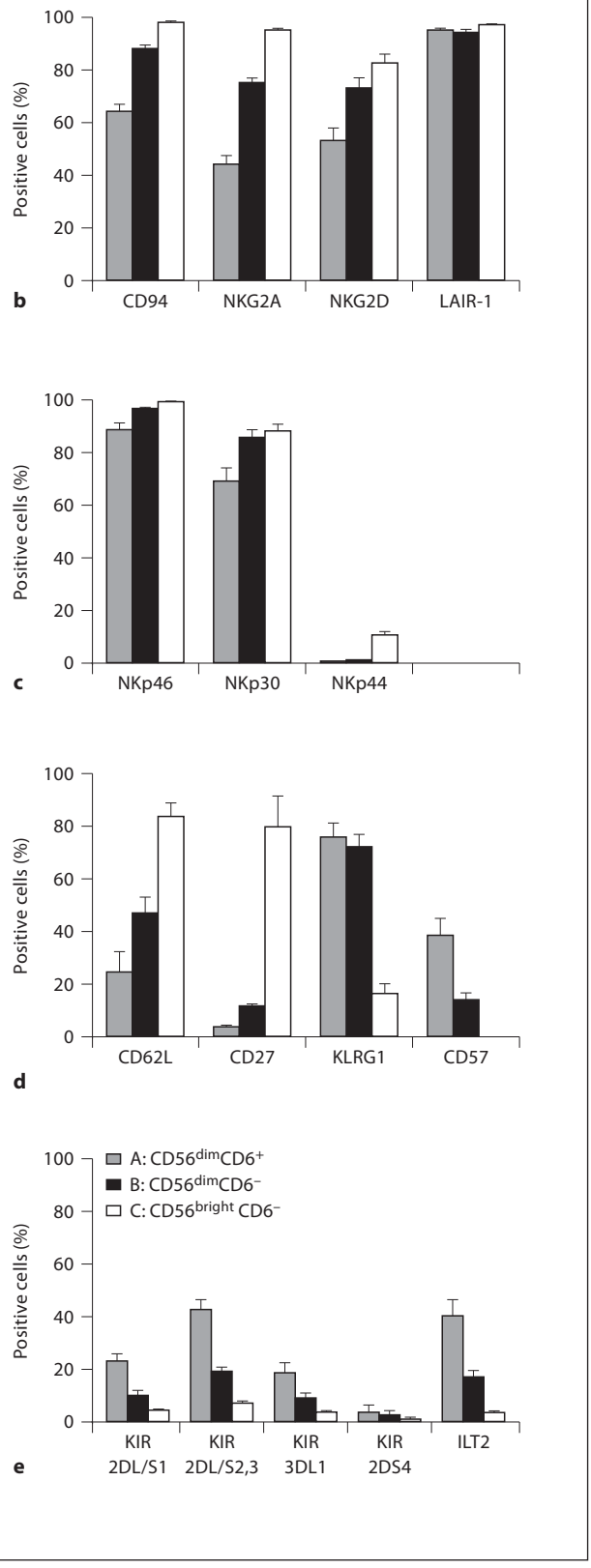


**Fig. 2.** Extended phenotype of $CD6^+$ and $CD6^-$ NK cell subpopulations. Expression of NK-associated markers was analyzed on the 3 NK cell fractions classified by CD6 and CD56 expression, as depicted in figure 1. **a** Expression of CD94 and NKG2A in the 3 NK subsets A–C defined by CD6 of 1 representative donor. The percentages of highly positive cells are indicated. **b** Expression of C-type lectin family members CD94 (n = 13), NKG2A (n = 22), NKG2D (n = 10) and LAIR-1 (n = 10). Since these receptors are present on virtually all NK cells, the mean values represent cells with high receptor density. For statistics, the unpaired (2-sample) t test was applied. CD94 and NKG2A, $p < 0.0001$ (for each comparison); NKG2D, $p < 0.0074$ ($CD56^{bright}CD6^-$ vs. $CD56^{dim}CD6^-$, $p > 0.05$); LAIR-1, $p > 0.05$. **c** Expression of the 3 natural cytotoxicity receptors. Since virtually all NK cells are positive for NKp46 (n = 13) and NKp30 (n = 13), the data represent the mean values of $NKp46^{bright}$ and $NKp30^{bright}$ NK cells. NKp46, $p < 0.01$; NKp30, $p < 0.02$ ($CD56^{bright}CD6^-$ vs. $CD56^{dim}CD6^-$, $p > 0.05$); NKp44, $p < 0.0095$. **d** Expression of CD62L (n = 6), CD27 (n = 5), KLRG1 (n = 4) and CD57 (n = 13) that are differentially expressed by NK subsets A–C. CD62L, $p < 0.04$; CD27, $p < 0.0005$; KLRG1, $p > 0.48$ ($CD56^{dim}CD6^+$ vs. $CD56^{dim}CD6^-$) and $p < 0.03$ ($CD56^{dim}$ $CD6^+$ or $CD6^-$ vs. $CD56^{bright}$), and CD57, $p < 0.007$ (for each comparison). **e** Expression of KIR (n = 11–22) and ILT2 (n = 12), which are predominantly present on $CD56^{dim}$ NK cells and, within this subset, found on greater percentages of $CD6^+$ cells. KIR2DL/S1, KIR2DL/S2,3 and KIR3DL1, $p < 0.02$; KIR3DL1 $CD56^{dim}CD6^+$ versus $CD56^{dim}CD6^-$, $p = 0.053$; KIR2DS4, $p > 0.05$; ILT2, $p < 0.0023$. Bars indicate the mean percentages of highly positive NK cells within each fraction (±SEM). The percentages of positive cells and the numbers of analyzed donors for each marker are depicted in online supplementary table 1.

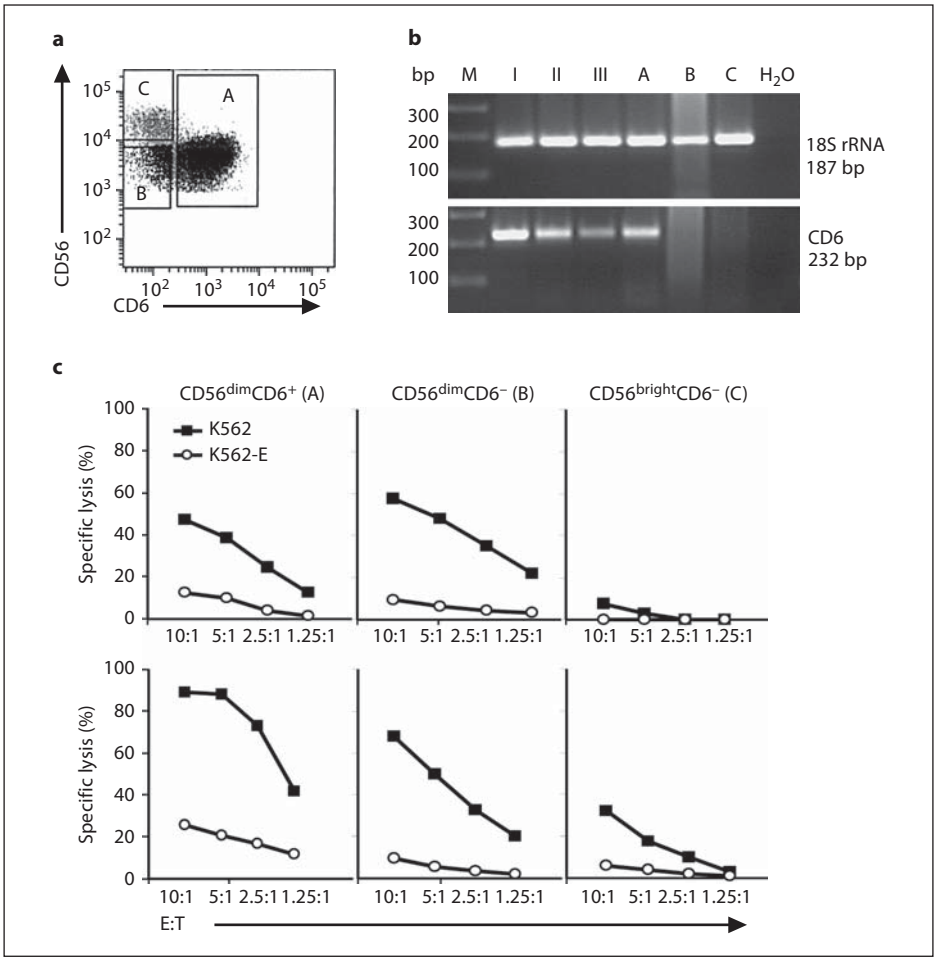


**Fig. 3.** CD6 transcripts are only detected in the $CD56^{dim}CD6^{+}$ NK subset and CD6 expression is irrelevant for cytotoxicity. Enriched NK cells were sorted by flow cytometry and the subpopulations were analyzed for CD6 transcripts. **a** According to the 3 NK cell fractions defined in figure 1a, the FACS sorting gates were set to avoid cross-contamination among the sorted subpopulations. **b** Analysis of CD6 transcripts by qRT-PCR. The housekeeping gene 18S rRNA served as a control for mRNA quantity and quality, whereas $H_2O$ served as a negative control. Lane I shows PBMC before NK isolation, lane II shows the NK cell-depleted fraction containing monocytes, T and B cells, and lane III shows enriched NK cells, including the 3 NK cell fractions. Lanes marked A, B and C show CD6 transcript expression for the respective NK cell fractions. CD6 transcripts are only amplified in fraction A, whereas they are missing in fractions B and C which correlates with the missing surface expression on the NK cell fractions as depicted in figure 1. **c** Cytotoxic activity of the 3 NK cell fractions against K562 and K562-E target cells. NK cells of 2 donors were sorted into 3 fractions according to the gating strategy shown in figure 3a and analyzed in standard chromium release assays for their cytotoxic potential against the HLA class I negative cell line K562 (■) and the HLA-E transfectant K562-E (○). We show the percentage of specific lysis of the target cells in 4-step titrations (E:T) mediated by the $CD56^{dim}CD6^{+}$, $CD56^{dim}CD6^{-}$ and C $56^{bright}CD6^{-}$ NK cell fractions, respectively.

the CD6 receptor on NK cells with plate-bound mab (clone MT-606) did not induce CD69 upregulation (data not shown) or degranulation by $CD56^{dim}$ cells which harbored the major fraction of $CD6^{+}$ NK cells (fig. 4d; online suppl. fig. 3). In contrast, both $CD56^{bright}$ and $CD56^{dim}$ NK cell subsets showed strong degranulation after mab-mediated triggering of activating receptors like CD16, NKp46 and NKp30, whereas weak degranulation was observed following stimulation via NKG2D, 2B4 and DNAM-1. NKG2C and NKp80 triggering did not induce degranulation. A possible coactivating function of CD6 regarding degranulation could be excluded since no increased CD107a surface levels were observed on $CD56^{bright}$ or $CD56^{dim}$ NK cells following stimulation of

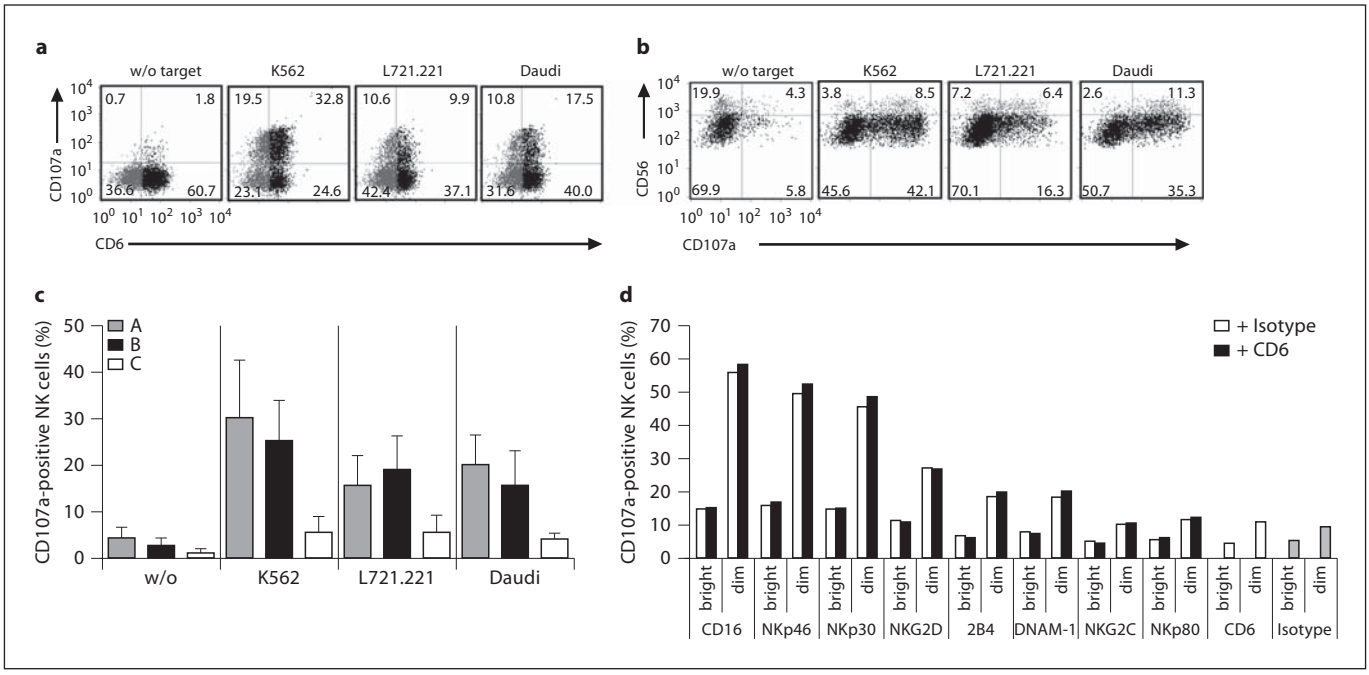


**Fig. 4.** Degranulation of NK cells is independent of CD6 expression and not induced by direct CD6 receptor stimulation. **a–d** Preactivated PBMC (500 U/ml IL-2, 48 h) were incubated with 3 different HLA class I negative target cells (**a–c**) or mabs against various activating NK receptors in combination with mab against CD6 (MT-606) or isotype control mab (**d**). The HLA class I negative target cells showed different expression of the CD6 ligand ALCAM (CD166): ALCAM$^+$ (Daudi, L721.221) and ALCAM$^-$ (K562; data not shown). Degranulation of NK cells was assessed by CD107a expression in the CD3$^-$CD56$^+$ NK cell subpopulation. **a**, **b** CD107a expression on CD3$^-$CD56$^+$ NK cells of PBMC of 1 representative donor in correlation with their CD6 expression (**a**) and their CD56$^{dim/bright}$ phenotypes (**b**), respectively. NK cells were incubated for 4 h with or without (w/o) target cells as negative control. Numbers indicate the percentages of NK cells in each quadrant. **c** Summary for NK cells of 13 healthy donors assessed for degranulation against these target cells. Depicted are the mean values of CD107a-positive cells for each NK cell fraction, calculated as percentages of total NK cells. The wide standard deviations reflect donor-specific variations in the overall NK cell degranulation potential ($p > 0.2$ for each combination, Mann-Whitney U test). **d** Degranulation of preactivated NK cells gated on CD56$^{bright}$ and CD56$^{dim}$ NK cells after 4 h of stimulation with receptor-specific mabs, with or without CD6. CD107a-positive NK cells are shown as percentage of all NK cells. The isotype control (grey bar) indicates the background of spontaneously degranulating (CD107a-positive) NK cells. White bars indicate stimulation with the receptor-specific mab in combination with isotype mab, and black bars show simultaneous stimulation of activating receptors in combination with CD6. We show 1 of 2 representative examples for coactivation analysis, and mab stimulation of CD6 receptor alone was performed with >5 donors.

these activating NK receptors in the presence of CD6 mab (fig. 4d, black bars) compared with stimulation of the various activating receptors alone (fig. 4d, white bars).

*CD6 Stimulation Contributes to Cytokine and Chemokine Profiles of NK Subsets*

Since CD6 expression on CD56$^{dim}$ NK cells did not influence degranulation and direct cytotoxicity, it was of interest to determine the role of CD6 expression regarding cytokine and chemokine secretion. An enrichment of CD6$^+$ NK cells by FACS sorting requires staining with CD6 mab, and this procedure alone could modulate cytokine or chemokine secretion. To avoid this, CD56$^{dim}$ NK cells were isolated from fresh PBMC samples using negative isolation procedures that left the populations of interest untouched, whereby the resulting NK cell fractions contained >60–80% CD6$^+$ NK cells. In order to investigate direct CD6-mediated cytokine and chemokine production, CD56$^{dim}$ NK cells were stimulated with CD6-specific plate-bound mab (MT-606) for 48 h in the presence of 100 U/ml IL-2. In addition to isotype control mab, a CD3-specific mab was included to measure potential activation of the small percentage of residual T cells present in the separated NK cell fractions (<3%, data not shown). In isolated T cells, stimulation of CD6 was unable to induce higher cyto-

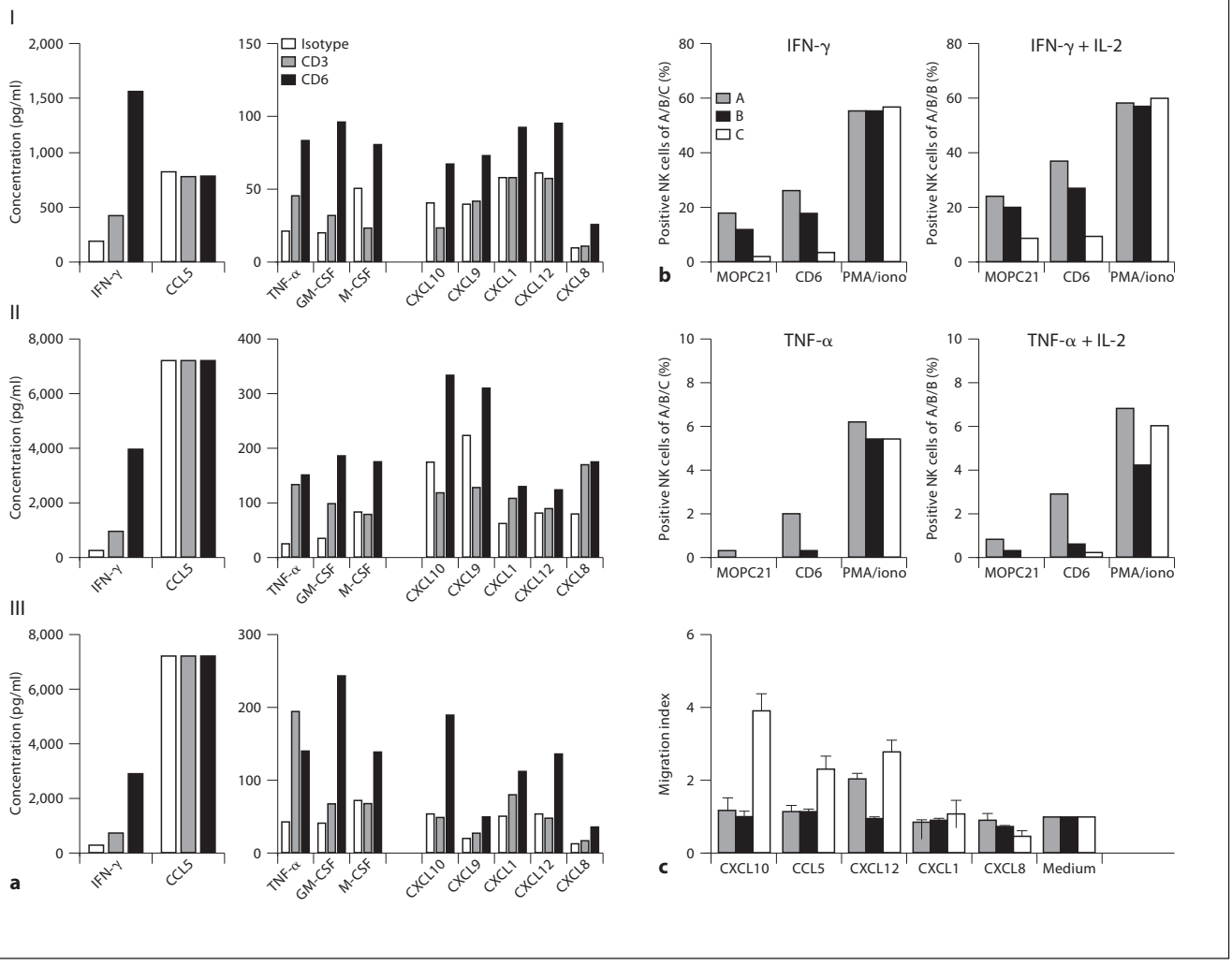


**Fig. 5.** CD6-mediated stimulation induces cytokine and chemokine secretion and $CD6^{+/-}$ NK cells have different migratory capacities towards chemokines. **a** Enriched $CD56^{dim}$NK cells (comprised of >60% $CD6^{+}$ cells) of 3 healthy donors (I–III) were stimulated with plate-bound specific mab against CD6 (clone MT-606, black bars) for 48 h in the presence of 100 U/ml IL-2. Isotype control mab (white bars) was included to detect spontaneous cytokine secretion, and CD3-specific mab (grey bars) served as an internal control for T-cell stimulation to assess activation of residual T cells (<3%, data not shown). Stimulation was performed with $5 \times 10^4$ (I) and $3 \times 10^5$ (II and III) $CD56^{dim}$ NK cells, respectively, and the supernatant was analyzed by the multiplex technology. Concentrations of cytokines IFN-γ, TNF-α, granulocyte macrophage colony-stimulating factor (GM-CSF), macrophage colony-stimulating factor (M-CSF) and chemokines CCL5, CXCL10, CXCL9, CXCL1, CXCL12 and CXCL8 are depicted in pg/ml. **b** Intracellular staining of IFN-γ (upper panel) and TNF-α (lower panel) following 6 h of stimulation via isotype mab MOPC21, CD6 mab (MT-606) or PMA/ionomycin (PMA/iono) with (right panel) or without (left panel) IL-2 (500 U/ml). The percentages of IFN-γ or TNF-α-positive NK cells were calculated for NK subsets A–C upon gating on $CD3^{-}CD56^{+}$ NK cells. **c** Migration of NK cell subsets towards chemokines was assessed in transwell experiments using 100 ng/ml for each chemokine or medium with 0.5% BSA with or without FBS as reference in the lower chamber. After 4 h, cells were harvested in the lower chamber and stained for CD56 and CD6; cell numbers were adjusted by counting 5,000 beads, and the medium/BSA control was set as migration index of 1 for each NK subset (A–C). According to these background migration values, the numbers of migrating cells in response to the chemokines are expressed as an x-fold migration index.

kine levels than stimulation of CD3 (not shown). Several cytokines and chemokines were quantified in the supernatant using the protein multiplex technology. The results of 3 donors (I–III) are shown in figure 5a. Stimulation via CD6 induced strong secretion of IFN-γ and weak secretion of TNF-α as well as production of several chemokines, like CXCL10 (IP-10), CXCL9 (MIG), CXCL1 (GRO-α), CXCL12 (SDF-1α) and CXCL8 (IL-8) at levels above the isotype and CD3 background control. Interestingly, secretion of CCL5 (RANTES) was inducible by IL-2 and could be enhanced by additional CD6 triggering in some donors (online suppl. fig. 4A). A direct comparison of 3 CD6-specific mabs with or without IL-2 revealed that MT-606-mediated stimulation resulted in a more effective secretion of IFN-γ and TNF-α compared with the other 2 mabs, MEM-89 or BL-CD6 (online suppl. fig. 4A). In general, addition of IL-2 strongly supported CD6-mediated cytokine secretion. To demonstrate the capability of CD6 to trigger cytokine and chemokine production directly, we performed ICS for IFN-γ, TNF-α and CXCL10 (IP-10). Low percentages of spontaneously IFN-γ-producing NK cells were detected in subsets A ($CD6^+CD56^{dim}$) and B ($CD6^-CD56^{dim}$) but not in subset C ($CD6^-CD56^{bright}$) in unstimulated NK cells after 6 h of incubation with isotype control mab (MOPC21; fig. 5b). Triggering of CD6 via mab MT-606 slightly increased the number of IFN-$\gamma^+$ NK cells in subset A, especially in the presence of IL-2. In contrast, unspecific stimulation with phorbol myristate acetate (PMA)/ionomycin induced high numbers of IFN-$\gamma^+$ NK cells in all 3 NK cell subsets. Generally, lower numbers of TNF-α-producing NK cells were observed even with PMA/ionomycin stimulation. However, CD6 stimulation with mab MT-606 induced TNF-α exclusively in the $CD6^+CD56^{dim}$ subset A in a less IL-2-dependent manner compared with IFN-γ. Since CXCL10 (IP-10) represents a classical downstream target of the IFN pathway, it was expected that direct stimulation via CD6 or even with PMA/ionomycin would not be able to induce CXCL10 in any NK cell subset (online suppl. fig. 4B). However, some CXCL10 $(IP\text{-}10)^+$ NK cells could be detected in $CD6^+CD56^{dim}$ NK cells (subset A) after 6 h of stimulation with CD6 mab in the presence of IFN, which strongly supported an IFN-dependent pathway for the production of CXCL10 (IP-10) in $CD6^+$ NK cells.

Finally, we investigated the migratory behavior of the NK subsets A–C in response to the chemokines which are produced by NK cells themselves (fig. 5c). Within 4 h, migration of $CD6^-CD56^{bright}$ NK cells (subset C) was induced by the CXCR3 ligand CXCL10 (IP-10) and to a lesser extent by the CCR5 ligand CCL5 (RANTES), which nicely confirms published data on CXCR3 and CCR5 expression by the $CD16^-CD56^{bright}$ NK cell subset. In contrast, CXCL12 (SDF-1α) induced migration of $CD6^+CD56^{dim}$ (subset A) and $CD6^-CD56^{bright}$ (subset C) NK cells but not $CD6^-CD56^{dim}$ (subset B) NK cells, indicating that CD6 may also serve as a marker for $CD56^{dim}$ NK cells with a different migratory capacity. Interestingly, neither of the 2 CXCR1/2 ligands CXCL1 (GRO-α) or CXCL8 (IL-8) was able to induce migration of $CD56^{dim}$ NK cells, although both $CD56^{dim}$ subsets are reported to express the respective chemokine receptor [1].

## Discussion

Peripheral human NK cells can be divided into 2 major subsets by their expression density of CD56, giving rise to $CD56^{dim}$ and $CD56^{bright}$ cells, which are associated with different functions. Here, we could show that the $CD56^{dim}$ subset can be further subdivided by the expression of CD6 which is accompanied by a functional difference in cytokine/chemokine secretion. Within peripheral $CD56^{dim}$ NK cells of healthy donors, a significantly greater NK fraction was $CD6^+$, reaching a mean value of 70.5%. The donor-specific variation in the percentage of $CD6^+$ cells is independent of freezing/thawing procedures. In stringently sorted cells, CD6 transcript expression correlated with surface receptor expression, since CD6 transcripts were not detected in NK cells with the $CD56^{dim}CD6^-$ phenotype, nor were they found in $CD56^{bright}$ cells. In activated human T cells, different CD6 splice variants have been reported, whereby either the ALCAM-binding SRCR3 domain (exon 5) and/or cytoplasmic regions (exons 8 and/or 9 and 12) are deleted [22, 23]. Upon T-cell activation, the full-length CD6 mRNA is replaced by these splice variants. This alteration was also detectable in NK cells in which the full-length mRNA dominated in freshly isolated NK cells and decreased substantially upon IL-2 activation, whereby shorter amplicons appeared (online suppl. fig. 1B). This observation indicates a similar activation-dependent mRNA regulation of CD6 in human T and NK cells. These splice variants could not be distinguished at the surface since all available CD6-specific mab bind to the SRCR1 domain that is present in all isoforms carrying a transmembrane region [24].

Thus, both surface phenotype and molecular analysis allowed 3 NK fractions to be defined on the basis of CD6 expression and density of CD56 molecules:

$CD56^{bright}CD6^{-}$, $CD56^{dim}CD6^{-}$ and $CD56^{dim}CD6^{+}$. A similar expression pattern was recently shown for the C-type lectin receptor CD94 by the group of Caligiuri et al. [7], who demonstrated the existence of 3 peripheral NK subpopulations, $CD56^{bright}CD94^{high}$, $CD56^{dim}CD94^{high}$ and $CD56^{dim}CD94^{low}$. It was speculated that the $CD56^{dim}CD94^{high}$ fraction represents the phenotypic and functional intermediate in the differentiation process from $CD56^{bright}CD94^{high}$ to $CD56^{dim}CD94^{low}$ NK cells. Our analysis of the 3 NK subsets defined by CD6 revealed a correlation with the distribution based on the NKG2A/CD94 expression. NKG2A/CD94 was present at high density on virtually all $CD56^{bright}CD6^{-}$ and at a significantly lower density on $CD56^{dim}CD6^{+}$ NK cells, with the $CD56^{dim}CD6^{-}$ NK cells showing an intermediate expression level. This expression pattern may suggest that $CD6^{+}$ NK cells represent the more differentiated NK cell subsets within the $CD56^{dim}$ cells, which is supported by the observation that $CD6^{+}$ NK cells display a weaker proliferative capacity than $CD6^{-}$ NK cells in response to cytokine stimulation with IL-2 and IL-15, respectively (online suppl. fig. 6). Under these conditions, CD6 surface expression was not substantially modulated in $CD6^{-}$ and $CD6^{+}$ sorted NK cells (online suppl. fig. 2A).

Recent studies revealed that NK cells also differ with respect to the expression of homing receptors which influence their tissue distribution [1]. We found, in accordance with published data [12], that $CD56^{bright}CD6^{-}$ cells expressed the highest levels of CD62L (L-selectin), a critical lymphocyte homing receptor that regulates the migratory capacity and extravasation into tissues [1]. Interestingly, the reciprocal expression patterns of CD6 and CD62L on a large fraction of $CD56^{dim}$ cells may have an impact on the tissue distribution and cellular interactions with ALCAM-expressing cells, for instance endothelial cells, mature dendritic cells and synovial fibroblasts. In this context, it has been recently shown that ALCAM expression on blood-brain-barrier endothelium regulates the migration of $CD4^{+}$ T cells into the central nervous system [25], whereas the role of CD6 for NK cell migration still needs to be assessed.

Like CD62L, CD27, a member of the TNF receptor family, is highly expressed on $CD56^{bright}CD6^{-}$ NK cells and almost absent in the $CD56^{dim}$ subset. It has been recently shown that CD27 defines a functionally distinct NK subpopulation present within the $CD56^{bright}$ NK subset, whereas the absence of CD27 marks NK cells with higher perforin/granzyme B expression and cytotoxic potential [11]. We found a significant difference in CD27 expression between $CD6^{-}$ and $CD6^{+}CD56^{dim}$ NK cells ($p = 0.0001$), which was not directly correlated with a generally higher cytotoxicity of $CD6^{+}$ NK cells (fig. 3d, 4). This may be explained by the concomitant lower expression of various activating NK receptors in the $CD6^{+}$ subset such as NKG2D and NKp30. The difference in the cytotoxicity of the 2 $CD56^{dim}$ subsets ($CD6^{+}$ and $CD6^{-}$) seen in figure 3d might therefore be explained by donor-specific variations regarding the expression of activating receptors and CD27.

Further analysis of the 3 NK cell fractions revealed additional differences in the expression of various receptors that control the dynamic balance of NK activation. The expression of activating and inhibitory KIR and members of the ILT family is known to be restricted to the $CD56^{dim}CD16^{+}$ NK subset which was confirmed by our own analyses (online suppl. fig. 5) [2]. The majority of $KIR^{+}$ NK cells was found in the $CD56^{dim}CD6^{+}$ NK subpopulation, with a similar distribution of the KIR2DL/S1, KIR2DL/S2,3, KIR3DL1 and KIR2DS4 receptors (fig. 2e) independent from the KIR haplotypes of individual donors (data not shown), whereas $CD56^{bright}CD6^{-}CD94^{high}$NK cells were almost negative. The same expression pattern was observed for the inhibitory ILT2 receptor. The reciprocal distribution of KIR and C-type lectin inhibitory receptors on these NK cell subsets assures that tolerance to self-major histocompatibility complex is maintained by virtually all NK cells [3, 26]. The intermediate position of the $CD56^{dim}CD6^{-}CD94^{high}$ NK cells is again reflected by the expression levels of KIR and ILT2 that are in the range between those of $CD56^{dim}CD6^{+}$ and $CD56^{bright}CD6^{-}$ cells. Recently, the well-known CD57 marker was described as a potential maturation marker for NK cells defining a more differentiated subset within $CD56^{dim}$ NK cells [20, 21]. Therefore, it is not surprising that CD57 expression follows a similar distribution as KIR and ILT2 (fig. 2d). In contrast, the KLRG1 receptor which recognizes E- but not N-cadherin [27] is rather equally distributed in $CD6^{+}$ and $CD6^{-}$ NK cells but absent on the $CD56^{bright}$ NK cell subset.

All 3 NK fractions were mostly positive for the activating NK receptors NKG2D, NKp30 and NKp46, although variations in receptor density were observed, particularly with respect to NKG2D where many cells with lower expression density were found in the $CD56^{dim}CD6^{+}$ NK subset. NKp46 expression levels also varied among the fractions with the highest density found for $CD56^{bright}CD6^{-}$ NK cells. As expected, the activation-induced NKp44 receptor was almost absent on all 3 fractions of non-stimulated NK cells with the exception

of a small percentage of positive cells found within the $CD56^{bright}$ fraction.

Regarding cytotoxicity, $CD56^{dim}CD6^{+}$ and $CD56^{dim}$ $CD6^{-}$ NK cells showed a higher specific lysis of K562 than $CD56^{bright}CD6^{-}$ cells. This is in accordance with published data of the cytotoxic potential of resting NK cells [28]. The presence of CD6 on $CD56^{dim}$ NK cells does not correlate with a higher intrinsic natural cytotoxicity, as both $CD56^{dim}CD6^{-}$ and $CD56^{dim}CD6^{+}$ showed comparable killing of K562 target cells. This confirms published data for the $CD94^{high}$ and $CD94^{low}CD56^{dim}$ NK cells as well as for $CD57^{-}$ and $CD57^{+}CD56^{dim}$ NK cells, where no difference in natural cytotoxicity among the 2 fractions could be detected irrespective of the higher intracellular granzyme B/perforin expression in $CD94^{low}$ and $CD57^{+}$ NK cells [7, 20]. Irrespective of the density of NKG2A/CD94 expression, both $CD6^{+}$ and $CD6^{-}$ $CD56^{dim}$ cells were strongly inhibited in their killing of K562-E target cells via the interaction of the inhibitory NKG2A/CD94 receptor complex with HLA-E molecules expressed by the target cells (fig. 3d) [15, 16, 29].

These results were confirmed by degranulation assays using activated NK cells and additional HLA class I negative target cells that show different CD6 ligand (ALCAM) expression. There was no significant difference in degranulation of $CD56^{dim}CD6^{-}$ or $CD56^{dim}CD6^{+}$ NK cells ($p > 0.2$), indicating that the expression of ALCAM on Daudi and L721.221 cells had no impact on the activation of $CD6^{+}$ NK cells. Moreover, direct stimulation of CD6 receptors on NK cells by antibody cross-linking caused neither degranulation (fig. 4D) nor proliferation (data not shown). The possibility of CD6 serving as a coactivating receptor was also excluded since the degree of degranulation in NK cells was not changed by stimulation of activating NK receptors in combination with CD6. These results demonstrate that there was no intrinsic difference in the cytotoxic potential of $CD6^{+}$ and $CD6^{-}$ NK cells, and activation of the CD6 receptor had no apparent impact on NK cytotoxicity.

In contrast, CD6 appeared to influence the secretion of certain cytokines and chemokines, including IFN-γ, TNF-α, granulocyte macrophage colony-stimulating factor, CXCL10 (IP-10) and CXCL-9 (MIG), especially in the presence of IL-2 that may serve as a costimulatory pathway for CD6-mediated signals (fig. 5a; online suppl. fig. 4A). The direct capability of the CD6 receptor to induce cytokines was demonstrated by ICS that confirmed the costimulatory role of IL-2 for IFN-γ rather than for TNF-α (fig. 5b). The $CD6^{+}CD56^{dim}$ NK subset A showed a higher proportion of cytokine-producing cells compared with the other subsets, especially with respect to TNF-α. As expected, CXCL10 secretion could neither be induced directly via CD6 nor via PMA/ionomycin (online suppl. fig. 4B). However, in the presence of IFN signaling, CXCL10 production became detectable, suggesting that the high CXCL10 secretion seen in IL-2-preactivated NK cells is likely to be a consequence of the CD6-mediated IFN-γ secretion. CXCL10 and CXCL9 are ligands for the CXCR3 chemokine receptor which is expressed at high levels on $CD56^{bright}$ and in lower density on $CD56^{dim}$ NK cells [1]. Together with other CD6-induced chemokines, like CXCL1 (GRO-α) and CXCL12 (SDF-1α) which support the migration of $CXCR2^{+}$ and $CXCR4^{+}$ NK cells as well as T cells to sites of inflammation, this CD6-mediated chemokine secretion is likely to influence the inflammatory response through the recruitment of NK and other immune cells. Therefore, we investigated the migratory capacity of our NK subsets A–C in response to a selection of those chemokines that are inducible via CD6, i.e. CXCL10, CCL5, CXCL12, CXCL1 and CXCL8 (fig. 5c). A different migratory activity was observed in NK subsets A–C according to their published chemokine receptor expression. Only $CD6^{-}CD56^{bright}$ NK cells (subset C) expressing CXCR3 and CCR5 migrated towards CXCL10 and CCL5 gradients which nicely fits to the published expression pattern for human and murine NK cells [1]. Interestingly, only the $CD6^{+}$ (subset A) but not the $CD6^{-}$ (subset B) fraction of $CD56^{dim}$ NK cells migrated towards the CXCR4 ligand CXCL12 together with $CD6^{-}CD56^{bright}$ NK cells (subset C). In contrast, neither CXCL1 nor CXCL8 were able to induce migration of any of the 3 NK subsets although both receptors are found on the surface of NK cells (data not shown). This difference between $CD6^{+}$ and $CD6^{-}$ $CD56^{dim}$ NK cells in migration towards the CXCR4 ligand CXCL12 implies a differential response to chemokines despite the presence of the cognate receptor. These observations may explain a phenomenon that we found in a human tumor setting (unpublished data). In human colorectal tumor tissue, NK cells are extremely rare despite the presence of a chemokine gradient of CXCL1, CXCL8 and others from normal colon towards tumor tissue. Thus, a poor responsiveness of NK cell subsets to chemokines may be counterproductive in the tumor setting where NK cells may be necessary as additional effector cells in order to control tumor growth. In summary, our studies reveal that CD6 receptor expression on NK cell subpopulations has no impact on cytotoxicity but is capable of inducing cytokine secretion. Therefore, it can be assumed that CD6 expression on a large fraction of

$CD56^{dim}$ cells may help to select and shape the microenvironment in which these NK cells act as conductors of proinflammatory conditions. First, it may influence tissue localization of $CD56^{dim}CD6^{+}$ cells through interactions with ALCAM-expressing cells. Second, it may shape the microenvironment through subtle selective chemokine secretion that occurs via CD6 receptor triggering. This, in turn, could influence the recruitment of additional players in a local immune response. Altogether, these activities would support both amplification of innate immunity and induction of adaptive immune responses.


## Acknowledgments

We thank Stefan Maßen and Christian Quack for their statistical support. This study was supported by the Helmholtz Alliance 'Immunotherapy of Cancer' (M.B., D.J.S., C.S.F.), grant III/3 of the Tumor Center Heidelberg/Mannheim (C.S.F.), program project grant 'Tumor Therapy by Allogeneic Transplantation' of the German Cancer Aid (D.J.S., C.S.F.) and grants of the German Research Council DFG, SFB455 (D.J.S.), SFB571 and TRR77 (C.S.F.).


## Disclosure Statement

The authors declare no competing financial interests.

## References


1 Gregoire C, Chasson L, Luci C, Tomasello E, Geissmann F, Vivier E, Walzer T: The trafficking of natural killer cells. Immunol Rev 2007;220:169–182.

2 Cooper MA, Fehniger TA, Caligiuri MA: The biology of human natural killer-cell subsets. Trends Immunol 2001;22:633–640.

3 Anfossi N, Andre P, Guia S, Falk CS, Roetynck S, Stewart CA, Breso V, Frassati C, Reviron D, Middleton D, Romagne F, Ugolini S, Vivier E: Human NK cell education by inhibitory receptors for MHC class I. Immunity 2006;25:331–342.

4 Chan A, Hong DL, Atzberger A, Kollnberger S, Filer AD, Buckley CD, McMichael A, Enver T, Bowness P: $CD56^{bright}$ human NK cells differentiate into $CD56^{dim}$ cells: role of contact with peripheral fibroblasts. J Immunol 2007;179:89–94.

5 Romagnani C, Juelke K, Falco M, Morandi B, D'Agostino A, Costa R, Ratto G, Forte G, Carrega P, Lui G, Conte R, Strowig T, Moretta A, Munz C, Thiel A, Moretta L, Ferlazzo G: $CD56^{bright}CD16-$ killer Ig-like receptor-NK cells display longer telomeres and acquire features of $CD56^{dim}$ NK cells upon activation. J Immunol 2007;178:4947–4955.

6 Loza MJ, Perussia B: The IL-12 signature: NK cell terminal $CD56^{+high}$ stage and effector functions. J Immunol 2004;172:88–96.

7 Yu J, Mao HC, Wei M, Hughes T, Zhang J, Park IK, Liu S, McClory S, Marcucci G, Trotta R, Caligiuri MA: CD94 surface density identifies a functional intermediary between the $CD56^{bright}$ and $CD56^{dim}$ human NK cell subsets. Blood 2010;115:274–281.

8 Singer NG, Richardson BC, Powers D, Hooper F, Lialios F, Endres J, Bott CM, Fox DA: Role of the CD6 glycoprotein in antigen-specific and autoreactive responses of cloned human T lymphocytes. Immunology 1996;88:537–543.

9 Aruffo A, Bowen MA, Patel DD, Haynes BF, Starling GC, Gebe JA, Bajorath J: CD6-ligand interactions: a paradigm for SRCR domain function? Immunol Today 1997;18:498–504.

10 Koopman LA, Kopcow HD, Rybalov B, Boyson JE, Orange JS, Schatz F, Masch R, Lockwood CJ, Schachter AD, Park PJ, Strominger JL: Human decidual natural killer cells are a unique NK cell subset with immunomodulatory potential. J Exp Med 2003;198:1201–1212.

11 Vossen MT, Matmati M, Hertoghs KM, Baars PA, Gent MR, Leclercq G, Hamann J, Kuijpers TW, van Lier RA: CD27 defines phenotypically and functionally different human NK cell subsets. J Immunol 2008;180:3739–3745.

12 Frey M, Packianathan NB, Fehniger TA, Ross ME, Wang WC, Stewart CC, Caligiuri MA, Evans SS: Differential expression and function of l-selectin on $CD56^{bright}$ and $CD56^{dim}$ natural killer cell subsets. J Immunol 1998;161:400–408.

13 Juelke K, Killig M, Luetke-Eversloh M, Parente E, Gruen J, Morandi B, Ferlazzo G, Thiel A, Schmitt-Knosalla I, Romagnani C: CD62L expression identifies a unique subset of polyfunctional $CD56^{dim}$ NK cells. Blood 2010;116:1299–1307.

14 Ulbrecht M, Maier S, Hofmeister V, Falk CS, Brooks AG, McMaster MT, Weiss EH: Truncated HLA-G isoforms are retained in the endoplasmic reticulum and insufficiently provide HLA-E ligands. Hum Immunol 2004;65:200–208.

15 Falk CS, Mach M, Schendel DJ, Weiss EH, Hilgert I, Hahn G: NK cell activity during human cytomegalovirus infection is dominated by US2-11-mediated HLA class I down-regulation. J Immunol 2002;169:3257–3266.

16 von Geldern M, Simm B, Braun M, Weiss EH, Schendel DJ, Falk CS: TCR-independent cytokine stimulation induces non-MHC-restricted T cell activity and is negatively regulated by HLA class I. Eur J Immunol 2006;36:2347–2358.

17 Lebbink RJ, de Ruiter T, Adelmeijer J, Brenkman AB, van Helvoort JM, Koch M, Farndale RW, Lisman T, Sonnenberg A, Lenting PJ, Meyaard L: Collagens are functional, high affinity ligands for the inhibitory immune receptor LAIR-1. J Exp Med 2006;203:1419–1425.

18 Vitale M, Bottino C, Sivori S, Sanseverino L, Castriconi R, Marcenaro E, Augugliaro R, Moretta L, Moretta A: NKP44, a novel triggering surface molecule specifically expressed by activated natural killer cells, is involved in non-major histocompatibility complex-restricted tumor cell lysis. J Exp Med 1998;187:2065–2072.

19 Moretta A, Bottino C, Vitale M, Pende D, Cantoni C, Mingari MC, Biassoni R, Moretta L: Activating receptors and coreceptors involved in human natural killer cell-mediated cytolysis. Annu Rev Immunol 2001;19:197–223.

20 Lopez-Verges S, Milush JM, Pandey S, York VA, Arakawa-Hoyt J, Pircher H, Norris PJ, Nixon DF, Lanier LL: CD57 defines a functionally distinct population of mature NK cells in the human $CD56^{dim}CD16^{+}$ NK cell subset. Blood 2010;116:3865–3874.

21 Bjorkstrom NK, Riese P, Heuts F, Andersson S, Fauriat C, Ivarsson MA, Bjorklund AT, Flodstrom-Tullberg M, Michaelsson J, Rottenberg ME, Guzman CA, Ljunggren HG, Malmberg KJ: Expression patterns of NKG2a, KIR, and CD57 define a process of $CD56^{dim}$ NK cell differentiation uncoupled from NK cell education. Blood 2010;116:3853–3864.

22 Castro MA, Oliveira MI, Nunes RJ, Fabre S, Barbosa R, Peixoto A, Brown MH, Parnes JR, Bismuth G, Moreira A, Rocha B, Carmo AM: Extracellular isoforms of CD6 generated by alternative splicing regulate targeting of CD6 to the immunological synapse. J Immunol 2007;178:4351–4361.
23 Bowen MA, Whitney GS, Neubauer M, Starling GC, Palmer D, Zhang J, Nowak NJ, Shows TB, Aruffo A: Structure and chromosomal location of the human CD6 gene: detection of five human CD6 isoforms. J Immunol 1997;158:1149–1156.
24 Alonso R, Huerta V, de Leon J, Piedra P, Puchades Y, Guirola O, Chinea G, Montero E: Towards the definition of a chimpanzee and human conserved CD6 domain 1 epitope recognized by T1 monoclonal antibody. Hybridoma (Larchmt) 2008;27:291–301.
25 Cayrol R, Wosik K, Berard JL, Dodelet-Devillers A, Ifergan I, Kebir H, Haqqani AS, Kreymborg K, Krug S, Moumdjian R, Bouthillier A, Becher B, Arbour N, David S, Stanimirovic D, Prat A: Activated leukocyte cell adhesion molecule promotes leukocyte trafficking into the central nervous system. Nat Immunol 2008;9:137–145.
26 Valiante NM, Uhrberg M, Shilling HG, Lienert-Weidenbach K, Arnett KL, D'Andrea A, Phillips JH, Lanier LL, Parham P: Functionally and structurally distinct NK cell receptor repertoires in the peripheral blood of two human donors. Immunity 1997;7:739–751.
27 Rosshart S, Hofmann M, Schweier O, Pfaff AK, Yoshimoto K, Takeuchi T, Molnar E, Schamel WW, Pircher H: Interaction of KLRG1 with E-cadherin: new functional and structural insights. Eur J Immunol 2008;38:3354–3364.
28 Nagler A, Lanier LL, Cwirla S, Phillips JH: Comparative studies of human FcRIII-positive and negative natural killer cells. J Immunol 1989;143:3183–3191.
29 Braud VM, Allan DS, O'Callaghan CA, Soderstrom K, D'Andrea A, Ogg GS, Lazetic S, Young NT, Bell JI, Phillips JH, Lanier LL, McMichael AJ: HLA-E binds to natural killer cell receptors CD94/NKG2A, B and C. Nature 1998;391:795–799.